Materials and Design 193 (2020) 108673

Contents lists available at ScienceDirect

Materials and Design

journal homepage: www.elsevier.com/locate/matdes

Transparent model concrete with tunable rheology for investigating flow and particle-migration during transport in pipes

Günter K. Auernhammer [a,b], Shirin Fataei [c], Martin A. Haustein [d], Himanshu P. Patel [a], Rüdiger Schwarze [d], Egor Secrieru [c], Viktor Mechtcherine [c,*]

[a] Leibniz Institute of Polymer Research, Hohe Straße 6, 01069 Dresden, Germany
[b] Max Planck Institute for Polymer Research, Ackermannweg 10, 55128 Mainz, Germany
[c] TU Dresden, Institute for Construction Materials, Faculty of Civil Engineering, 01062 Dresden, Germany
[d] TU Bergakademie Freiberg, Institute of Mechanics and Fluid Dynamics, Lampadiusstr. 4, 09599 Freiberg, Germany

HIGHLIGHTS

- Highly transparent material developed is suitable for modeling concrete.
- Refractive indexes of the model fluid and glass particles could be well matched.
- Model "concrete" exhibits rheological behaviour similar to that of real concrete.
- Particle size distribution, solid content, and rheology of model concrete can be varied.
- Model concrete is suitable for studying particle migration during concrete pumping.

GRAPHICAL ABSTRACT

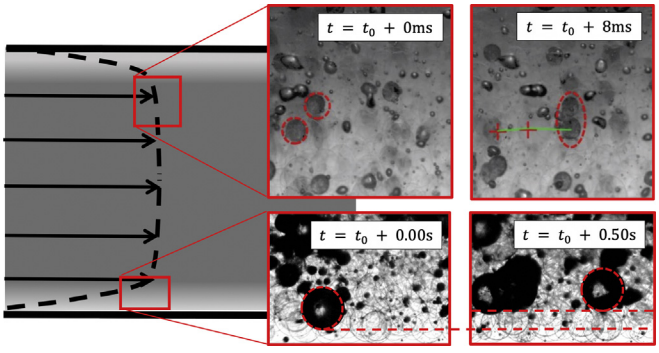

ARTICLE INFO

Article history:
Received 16 January 2020
Received in revised form 20 March 2020
Accepted 23 March 2020
Available online 7 May 2020

Keywords:
Granular suspensions
Construction materials
Fresh concrete
Particle migration
Refractive index
Rheometry

ABSTRACT

The article describes the adaption and properties of a model concrete for detailed flow studies. To adapt the yield stress and plastic viscosity of the model concrete to the corresponding rheological properties of real concrete, the model concrete is made of a mixture of glass beads and a non-Newtonian fluid. The refractive index of the non-Newtonian fluid is adjusted to the refractive index of the glass beads by the addition of a further constituent. The rheological properties of the model concrete are characterised by measurements in concrete rheometers. Finally, the first exemplary results from experiments with the model concrete are presented, which give incipient impressions of the complex internal dynamics in flowing concrete.

* Corresponding author.
E-mail addresses: auernhammer@ipfdd.de, *URL:* http://www.ipfdd.de/auernhammer (G.K. Auernhammer), ruediger.schwarze@imfd.tu-freiberg.de (R. Schwarze), viktor.mechtcherine@tu-dresden.de (V. Mechtcherine).

https://doi.org/10.1016/j.matdes.2020.108673

1. Introduction

Concrete is a very versatile building material used in a great variety of construction applications; in general it is also by far the most often used man-made material. From the scientific perspective, concrete is a multiphase, multiscale composite material consisting of mineral binders, water, sand, coarse aggregates, chemical admixtures and some air. In its fresh state, concrete exhibits many similarities to other very wet granular materials or very dense granular suspensions [1,12].

Processing fresh concrete is one of the keystones of modern construction technologies. In particular, the pumping of concrete is of high relevance since it is widely used for conveying concrete both on-site and, increasingly, also in precast plants. Furthermore, pumping is a central technological step in such emerging technologies as 3D-concrete-printing. Mastering the pumping of concrete and other processing stages demands a thorough understanding of concrete rheology. In this article the authors address pumping as a representative production step. Usually rheological behaviour of fresh concrete is described based on the Bingham model. While the determination of the model's parameters – yield stress and plastic viscosity – is not at all trivial for such a complex material as fresh concrete, it is even more challenging to characterise and eventually to predict its response under typical processing conditions; here, it means simply: during pumping. The main reasons for these difficulties are complex phenomena including shear-induced particle migration, segregation and the formation of a lubricating layer at the walls of the pumping pipeline [2,7,16,18]. These phenomena exert a major influence on processing performance; hence, their deeper understanding is of great importance to the further development of advanced concrete technologies. In general, the rheology of dense suspensions is very complex, which is shown in the excellent review of Morris et al. [21]. Unfortunately, real concrete cannot be investigated directly with common optical flow measurement techniques due to the opacity of fresh concrete.

In the last decade, transparent model materials have been suggested to monitor and analyze internal phenomena in detail during the processing of fresh concrete [3,4,17,22,24]. For example, Boulekbache et al. [4] investigated the movement of fibres in polyacrylic acid (Carbopol®) solution, which was applied as a model material representing fresh concrete. Spangenberg et al. [24] performed model experiments in order to investigate particle migration during a typical casting operation. Their model concrete was a mixture of a Carbopol® solution, which mimicked fine mortar, and glass beads of some millimeters in diameter representing coarse aggregates. Further, Bian et al. [3] demonstrated that model concretes made of Carbopol® and glass beads exhibited similar rheological behaviour and flow morphology as real fresh concrete. Additionally, Koch et al. [17] showed that such model concretes are also able to represent rheological behaviour of real fresh concrete under vibrational agitation.

Refractive index matching (RIM) is a well-established technique for analyzing high-concentrated suspensions [9,25–27]. However, there are very few studies on refractive index matching for suspensions based on non-Newtonian liquids. Zade et al. recently proposed an interesting approach with RIM for soft particles dispersed in a Carbopol gel with volume fractions up to 10% [28]. However, this model material is not suited to model a real concrete, because of the significantly higher solid-fraction of hard particles in concrete. Note that collisions of the non-deformable particles play an important role in segregation and migration processes.

The aim of the work at hand is to extend markedly the features of transparent model concretes made of Carbopol® and glass beads. In particular, in contrast to previous investigations, an approach which enables a quantitative characterisation of flow is suggested. It allows the separate quantification of the internal flow fields of both main concrete constituents – the binder paste or fine mortar and the aggregates – separately. For this purpose, the refractive indices of all materials in the model concrete and the boundary geometries, i.e., Carbopol®, glass beads and pipeline walls must be matched in addition to their rheological properties. Proper index matching makes the complete system transparent, allowing the investigator to follow the motion of tracer particles even far away from the pipe walls.

The outline of the paper is as follows: In Section 2, the materials employed and the methods for tuning the material parameters of the model concrete are given. Section 3 explains specific requirements with respect to the optical accessibility of the concrete flow region. Finally, the first experimental results obtained using pumping and flow setups are presented in Section 4.

2. Background

A model cement paste and a model concrete should meet the relevant rheological features of real fresh cement and fresh concrete, e.g., their non-Newtonian flow behaviour, as accurately as possible. In the study at hand these model systems should also allow for optical access to the near-wall and bulk flow regions without any distortion. This feature is necessary for local non-intrusive flow measurements, e.g. employing particle image velocimetry or particle tracking for the evaluation of segregation and other internal flow phenomena in the materials.

A key challenge in formulation of the model's materials is imposed by chemical reactions and hydration, both of which take place in the real materials. These processes introduce, among others, thixotropic flow behaviour of the cement and concrete. Such complex chemical reactions cannot be precisely reproduced in transparent model materials. Therefore, the rheological properties are considered time-independent for this study. Note that the time independence of model materials is their great advantage in comparison to real concrete since it enables measurements under well-controlled conditions. Such measurements can also deliver a data basis for calibration of numerical models for simulating of concrete.

With the assumption of time-independent properties, the formulation of the model materials is as follows: First, the rheological data of a specific real cement paste or fine mortar and a specific real concrete are analyzed in detail. Second, a composition of transparent model materials is designed, which gives enough flexibility in the formulation to reproduce the needed optical and relevant rheological properties, e.g., index matching and Bingham or Herschel-Buckley flow behaviour. The composition is then properly tuned in order to mirror the rheological data of the selected real materials. The additives needed for the index matching in the liquid part of the model system have a pronounced influence on the rheological properties. For this reason the second step includes the fine-tuning of the refractive index and the rheological properties in a combined optimization procedure. In the final step the rheological data of the model cement paste or fine mortar and model concrete are measured in detail. The comparison of the data from both the real and the model materials must provide proof of the proper choice of the model material formulations.

The goal here is not to copy all the rheological properties of real concrete in a transparent model system. Instead, we design a model system that shows the essential features of real concrete, e.g., a Bingham fluid with yield stress and plastic viscosity. Such a system allows the study of the basic mechanisms dominating the concrete flow behaviour by optical observation of the single-particle motion.

3. Designing the model concrete

Concrete is a dense polydisperse suspension, composed of water, cement and other fines, admixtures, fine sand, and coarse aggregates. To reduce the complexity that arises due to the broad particle size distribution, the particles finer than a specific threshold, e.g., 0.4 mm, are considered part of the homogenous carrier fluid in this investigation, and the particles coarser than the specific threshold are the suspended solid phase representing aggregates. Thus, possible flow-induced

redistribution and migration for particles finer than the specific threshold are neglected in our approach. To study the concrete flow behaviour and flow-induced migration of particles coarser than the specific threshold, e.g., 0.4 mm, a transparent non-Newtonian model concrete with tunable rheological properties is designed. The model concrete consists of a selected set of large transparent particles and a transparent non-Newtonian model fluid with the same refractive index as of the glass beads. i.e., the refractive index of model fluid is increased to match that of glass beads. Furthermore, translucent tracer particles with non-matching refractive index are added for tracking the flow in the model concrete. The authors use transparent glass particles of various diameters, representing the fine sand and coarse aggregates. The size range of the particles generally depends on the geometry of the testing setup. The model fluid should be designed to mimic the rheological properties of cementitious mortar with a maximum particle size smaller than the selected glass particles. This procedure implies that the rheological properties of the model fluids are a function of the size of the glass particles used.

3.1. Materials and mixture design for concrete

As described above, the main objective of this work is to design a tunable model concrete consisting of a transparent non-Newtonian model fluid and index-matched spherical glass particles that exhibits rheological properties similar to cementitious concrete. Three mixtures of conventional vibrated concrete (CVC) containing different volume fractions of coarse aggregates, i.e., larger than 1 mm, were designed and tested by the TUD group [10]. Table 1 presents the compositions of the target concretes and the required dosages of the constituents in kg for producing 1 m^3 of concrete. CEM III/A 42.5 N is the cement type according to DIN EN 197-4. The sand and gravel are differentiated using the minimum and maximum grain size in mm, according to DIN EN 12620. The concrete mixtures are limited to CVC with consistency class between F3 and F6, according to DIN EN 206-1. The class F6 refers to concrete mixtures with very flowable consistency (not yet self-compacting).

In the labelling of the samples, "C" represents concrete mixture and the following number indicates the volume fraction of coarse aggregates, >1 mm; for example, C42 corresponds to the concrete containing 42 vol% coarse aggregates. The volume fraction of each aggregate group, including quartz powder and fine sands, was chosen so that all together the aggregates matched the middle grading curve, according to DIN 1045-2. For simplicity, the constitutive fine mortar with a maximum aggregate size of 1 mm and the coarse aggregates larger than 1 mm are referred to as "mortar" and "aggregates", respectively. After mixing, the constitutive mortar was sieved out of concrete using a mesh opening size of 1 mm. The flow table tests were performed both on concrete (DIN EN 12350-5) and constitutive mortar (DIN EN 459-2), simultaneously with the rheological measurements. For flow table tests, a concrete/mortar cone is positioned on the center of the testing plate and it is filled in two successive layers to ensure full-filling of the cone. The upper radius/lower radius/height of the cones for concrete and mortar are 130/200/200 mm and 70/100/60 mm, respectively. 30 s after the cone is filled, it is lifted up and the concrete/mortar spreads depending on its rheological properties. Then, 15 strokes are applied to the sample by lifting and releasing the testing plate. The height of each stroke is 40 mm for concrete and 10 mm for mortar. Finally, the maximum and minimum radii that of the spread concrete/mortar are measured and the average is reported as the result, see Table 1.

Table 1
Concrete constituents and their dosage for production of 1 m^3 of concrete [10]. Cement type and grains' fractions are, according to DIN EN 197-4 and DIN EN 12620, respectively.

Materials		Density [kg/m^3]	Dosage [kg]		
			C42	C47	C52
Constit. mortar	CEM III/A 42.5 N	2990	425	388	351
	Quartz powder	2680	57	52	47
	Quartz sand 0.06–0.2	2650	57	52	47
	Quartz sand 0–1	2650	456	416	376
	Water	1000	211	192	173
	Superplasticizer	1056	3.48	3.18	2.87
Aggregate	Quartz sand 1–2	2650	210	235	260
	Quartz sand 2–4	2650	210	235	260
	Quartz gravel 4–8	2650	290	325	360
	Quartz gravel 8–16	2650	403	451	500
w/b [−]			0.50	0.50	0.50
SP % bwoc			0.72	0.72	0.72
Vol. agg. (>1 mm) [%]			42	47	52
Concrete flow table [mm]			640	545	450
Mortar flow table [mm]			260	260	240

3.2. Rheological parameters for mortar and concrete

The rheological properties of concrete bulk were determined using the wide coaxial gap concentric cylinder viscometer ConTec 5 (ConTec, Iceland [15]): see Fig. 1a.

The constitutive mortar that was obtained from concrete by sieving method is considered as the homogeneous fluid that carries the coarse solid particles, i.e., sand and aggregates in the concrete suspension. The HAAKE MARS II rheometer (Thermo Fisher Scientific, Germany [20]) was used to determine the rheological parameters of the mortar with a special measuring cell for building materials [20]; see Fig. 1b. The testing protocol consisted of a rate-controlled hysteresis loop with the maximum rotational velocity of 0.624 and 0.523 rps for ConTec 5 and HAAKE MARS II, respectively. The rotational velocity changed step-wise and in each step the torsional moment is recorded when a stationary value is reached.

Fig. 2 illustrates the flow curves obtained for conventional mortar and concrete. The output data of these devices is the torsional moment induced by the material vs. the rotational/angular velocities (N). In the case of Bingham-type flow curves for the ConTec 5 viscometer, the Reiner-Riwlin equations could be used to derive yield stress and plastic viscosity [11,14,23].

$$T = G + H \cdot N$$

$$\tau_0 = \frac{G}{4\pi h}\left(\frac{1}{R_i^2} - \frac{1}{R_0^2}\right)\frac{1}{\ln(R_0/R_i)}$$

$$\mu = \frac{H}{8\pi^2 h}\left(\frac{1}{R_i^2} - \frac{1}{R_0^2}\right)$$

where G (Nm) and H (Nm/rps) are the intercept and slope of the T-N curves. R_i and R_0 denote the inner and outer radii of the sampling cell and h marks the height of the tested sample. In the case of the HAAKE MARS II rheometer, the device is calibrated using a Newtonian calibration oil. This method is called Affine-Translation (AT) and it is used for arbitrary geometry without analytical solutions [13]. Table 2 summarizes the rheological parameters, yield stress and plastic viscosity, approximated for mortar and concrete by fitting the data to the Bingham model.

3.3. Materials and mixture design for model fluid and model concrete

The three institutes involved in this study used different testing setups to investigate particle migration in the model concrete during flow through a pipe: TU Dresden (TUD), TU Bergakademie Freiberg (TUBAF) and Leibniz Institute of Polymer Research in Dresden (IPF). These setups differ in pipe diameter and type of flow. The sliding pipe rheometer at TUD represents the real-scale case [19]. This device uses

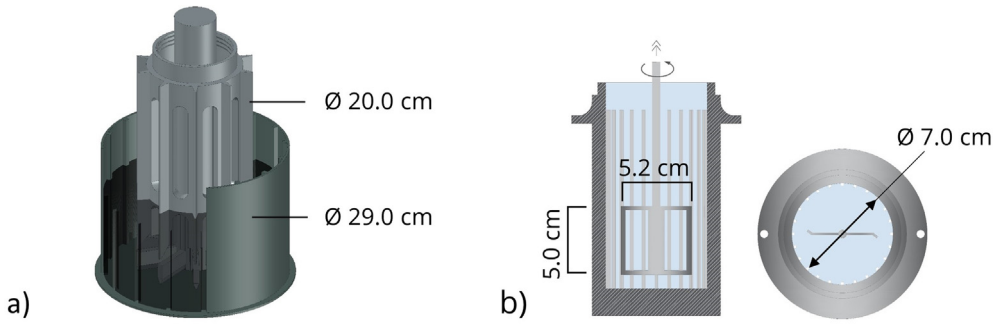

Fig. 1. a) Geometry of ConTec 5 viscometer, b) building material unit cell and rotor for HAAKE MARS II rheometer.

the particle size of its model concrete in the same range as of real concrete. The testing setups of TUBAF and IPF use pipe diameters that are, respectively, 1/6.25 and 1/3.4 times smaller than the ones at TUD. The setups with smaller pipe diameter use smaller borosilicate glass particles (Schäfer Glas GmbH, Germany) and a suitably adapted rheology of the model fluid; cf. Table 3 and the beginning of Section 3. This strategy also implies that the rheological properties of the TUBAF and IPF model concretes are not directly comparable to the real concrete. However, they can be compared to the TUD model concrete, which has similar rheological parameters to those of the real concrete.

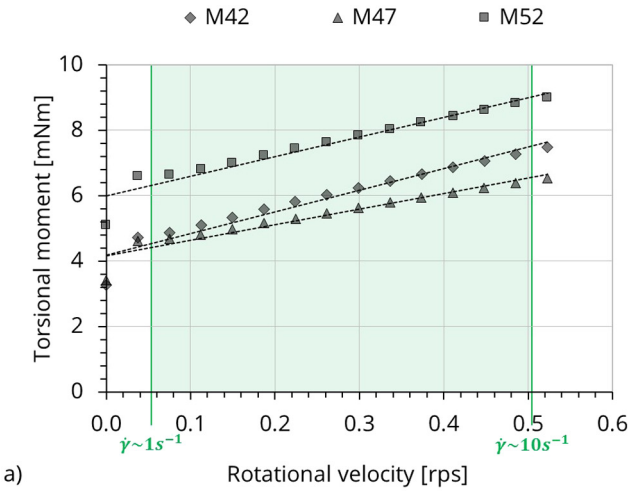

Fig. 2. Flow curves obtained for a) mortar and b) concrete compositions.

The following considerations were taken into account in designing the initial model concretes resulting in the mixture composition listed in Table 3:

- The total volume fraction of glass beads in model concrete is equal to total aggregates (>1 mm) of concrete mixtures;
- The combination of the different sizes of the glass beads must result in the maximum packing density of the cementitious system [8];
- The size of the glass beads is chosen according to the size of the testing setup (see Fig. 3):
  - TUD: 2, 4, 8 and 16 mm glass particles
  - IPF: 1 and 2 mm glass particles
  - TUBAF: 0.4–0.8 and 1 mm glass particles

- In the granular system of TUD, the maximum particle size and particle size distribution are adapted to that of the concrete composition;
- In the binary granular systems of IPF and TUBAF, the ratio between volume fraction of fine to coarse particles is 0.3/0.7;
- The rheological parameters of the model fluid should be modified according to each testing setup.

The model fluid has to fulfill two major requirements: (i) to mimic the rheological properties of cement paste and (ii) to match the refractive index of the larger particles. The non-Newtonian model fluid can be produced using standard viscosity-modifying polymer admixtures to water, e.g., Carbopol® or Carbomer®. The yield stress and plastic viscosity of these systems are tunable by adjusting the dosage and type of the polymer. We note that in cementitious materials the particles form a particle-particle network that, even if fragile, can still carry part of the weight of the larger particles. Since model fluid is actually single-phase and doesn't contain any finer particles, the yield stress of the fluid must be high enough to resist the segregation of the coarser particles. As discussed above, the rheological properties of the model fluid depend on how the originally broad particle size distribution is reflected in the threshold between model fluid and the glass particles. Accordingly, larger particle diameters and pipeline diameter require higher yield stress of the model fluid to prevent sedimentation of the particles.

Two types of model fluids were designed in the present study. A non-index-matching model fluid was produced at TUD to find the

Table 2
Rheological parameters for the investigated concrete mixtures.

Rheological parameters	C42	C47	C52
Concrete			
Yield stress [Pa]	65	120	270
Plastic viscosity [Pa·s]	19	25	37
Mortar			
Yield stress [Pa]	20.0	20.0	28.0
Plastic viscosity [Pa·s]	1.6	1.2	1.5

Table 3
Mixture compositions and the dosages for production of 1 m^3 of model concretes (MC) at three participating institutes.

Materials		Density [kg/m^3]	Dosage [kg]								
			TUD			IPF			TUBAF		
			MC42	MC47	MC52	MC42	MC47	MC52	MC42	MC47	MC52
Model fluid (MF)		1160	671	613	555	671	613	555	671	613	555
Glass beads	0.4–0.8 mm	2120	–	–	–	–	–	–	268	299	331
	1 mm	2120	–	–	–	268	299	331	624	699	773
	2 mm	2120	168	188	208	624	699	773	–	–	–
	4 mm	2120	168	188	208	–	–	–	–	–	–
	8 mm	2120	233	260	288	–	–	–	–	–	–
	16 mm	2120	323	362	400	–	–	–	–	–	–

suitable rheological parameters of the model fluid that can result in the targeted rheological parameters for the model concrete. This model fluid was produced by mixing Carbopol® EZ-2, distilled water and 18% wt. NaOH solution to adjust the pH level. The rheological investigation showed that for producing a model concrete similar to real concrete, the rheological parameters of its model fluid must be greater than those of the cementitious mortar; cf. Tables 2 and 5 for C42 and MC42-TUD, respectively.

The index-matching model fluid for tracking the particle experiments was produced for IPF and TUBAF. It was aimed at creating a model system that allows capturing the particle movement anywhere inside the pipe. This requires the full index matching of the model fluid and the glass particles and a suitable design of the experimental setup as well; cf. Section 4. It is worth mentioning that the samples must be free of air bubbles. The air bubbles' strong index-mismatching would hinder the observation of tracer particles.

The index-matching model fluid contains three components: water as carrier liquid, an index-matching additive (2,2-thiodiethanol, TDE) and a rheology modifier (Carbomer® TEGO ER 341). Since Carbopol® EZ-2 does not act as rheology modifier in water-TDE mixtures, Carbomer® TEGO ER 341 was found to be the best choice for this purpose. We note that all tested salts for matching the refractive index also turned out to be incompatible with the available viscosity modifiers. The water was prepared with an ultra-pure water device (ThermoFisher Branstead GenPure - Type1). TDE was purchased from Sigma-Aldrich (95% purity). Carbomer® TEGO ER 341 was kindly provided by Evonik. All chemicals were used as received from the supplier. The Carbomer® was mixed with an index-matching mixture of water and TDE. These substances were chosen to be suitable for tuning the rheology while being non-hazardous.

The refractive index n of the aqueous Carbomer® solutions is between ($n = 1.33$) and ($n = 1.35$). However, the refractive index of the glass beads is ($n \approx 1.473$). This difference is prohibitive for optical observation of internal dynamics in model concretes. TDE ($n = 1.521$) is used as an index-matching additive. In this work, the ratio for TDE: water was kept at 75:25, yielding $n = 1.473$, the refractive index of glass beads. As illustrated in Fig. 4, the sample is not completely transparent, probably due to slight inhomogeneities in the refractive index of the glass particles. A slight scattering of light is observed in the sample. However, opaque objects in the sample, like the tips of the tweezers shown in Fig. 4, are clearly visible at any position in the sample without considerable diffraction.

Table 4 summarizes the composition of the model fluids. The non-index matching model fluid with Carbopol® EZ-2 is marked as MF1 and the index-matching model fluid with Carbomer® TEGO ER 341 as MF2. This is due to these rheology modifiers' being optimized for aqueous systems, e.g., Carbopol® EZ-2, and slightly alcoholic systems, e.g., Carbomer® TEGO ER 341. These model fluids were used to produce model concrete with 42% volume concentration of glass particles; cf. MC42 in Table 3. The index-matching model fluid was produced with different Carbomer® concentrations of 0.8, 1.0 and 1.2 wt%. MF2-0.8% and MF2-1.2% were used in the model concretes produced for TUBAF and IPF, respectively, to attain the target rheological properties of the model concrete.

The mixing procedure plays a significant role in achieving a homogeneous and well-dispersed model fluid. In the present study, the mixing was performed using a Witeg Overhead Stirrer HT-DX (WITEG

Fig. 3. Transparent glass beads of different size ranging from 0.4 mm to 16 mm mimicking fine sand and coarse aggregates.

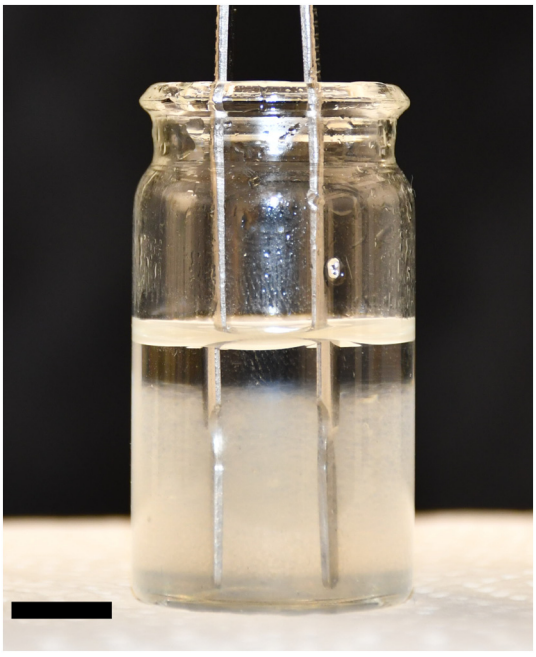

Fig. 4. Photograph of an index-matched sample. A slight scattering of the sample is visible. The scattering does not hinder the observation of opaque objects (e.g., the tips of the tweezers) in the sample. The scale bar is 15 mm.

Table 4
The compositions of the model fluids and the particle sizes used in the model concrete for TUD, IPF and TUBAF with 42% volume fraction of solid particles. The number in the notation indicates the amount of Carbomer® in the model fluid.

Institute	TUD	IPF	TUBAF
Notation of the model fluid	MF1-0.3%	MF2-1.2%	MF2-0.8%
Water [mass%]	100	25	25
2,2 thiodiethanol (TDE) [mass%]	–	75	75
Carbomer® 341 ER [mass%]	–	1.2	0.8
Carbopol® EZ-2 [mass%]	0.3	–	–
% wt. NaOH solution [mass%]	0.225	–	–
Particle size [mm]	2 to 16	1 & 2	0.4–0.8 & 1

Labortechnik GmbH, Germany). The following method for making model fluid is designed and developed by IPF group. A model fluid sample was prepared by first pouring 20% of the total volume of TDE into the mixing container. Then the total amount of Carbomer® was added on top of the liquid and the rest of the TDE (80% of the total volume) was poured into the container and on top of the Carbomer®. Thereafter, the sample is kept at rest for 2–3 h. In a further step, a stainless steel stirring rod of propeller geometry, with a rod length of 500 mm and a blade diameter of 50 mm, was used for stirring. For 48 h the sample was stirred at low speed in order to avoid air bubbles formation, in a closed container to prevent evaporation. Afterwards, the water was added. The sample was then stirred for another 5 days to allow homogeneous mixing of the Carbomer®, water and TDE. During this time, The stirring rate was adjusted to avoid the introduction of air bubbles and the container was kept closed to prevent evaporation. Finally, the prepared sample was stored in a cool and dark place.

The production of the index-matching model fluid requires a couple of additional considerations. To compensate minor changes in the refractive index due to the addition of Carbomer®, evaporation effects, or batch-to-batch variation of the materials, a small addition of either water or TDE might be needed to optimize the transparency of the final sample. It turns out that the most efficient mixture production is first to dissolve Carbomer® in TDE and only then to add water.

The glass beads are added in the ratio given in Table 3. The resulting sample is further stirred at a low shear rate to achieve the homogeneous distribution of the particles. Here, precautions must be taken to avoid the introduction of air bubbles. Otherwise, the particles can submerge with air voids between them cause light diffraction during the optical analysis.

3.4. Rheological parameters for model fluid and concrete

The model fluids containing different dosages of polymer and model concretes (except MC42-TUD) were rheologically investigated using the HAAKE MARS II rheometer. The flow curves are presented in Fig. 5. The MC42-TUD, with glass beads larger than 2 mm, was tested in the ConTec 5 viscometer. Additional measurements of the model fluids with an Anton Paar MCR 502 using a cone-plate geometry of diameter 50 mm and opening angle 1° showed the same tendencies with somewhat different absolute numbers. For better comparability of the rheological measurements on mortar, concrete and model concrete, we restrict the discussion here to the results obtained with the HAAKE MARS II rheometer and the ConTec 5 viscometer.

Different to the flow curves of cement paste and concrete, the flow curves of all model fluids do not show a linear regime in the range of rotational velocities in use; cf. Figs. 2 and 5a. Although the model fluids do not show a clear Bingham behaviour within the whole range of applied rotational velocities, they exhibit a close to linear behaviour within the rotational velocity range of 0.05–0.52 rps which corresponds to shear rate range of 1–10 s^{-1} in HAAKE MARS II rheometer. For a good comparability to the cementitious materials, the yield stress and plastic viscosity of the Bingham model are estimated for this range and compared

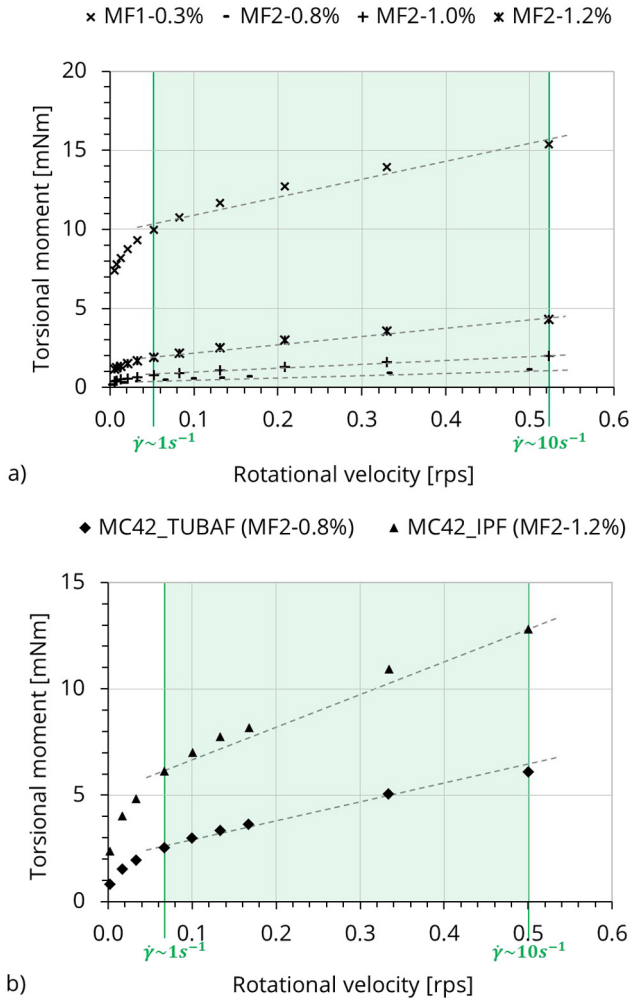

Fig. 5. Flow curve for a) model fluid containing different dosage of polymer, and b) model concretes investigated by IPF and TUBAF with 42% volume fraction of solids.

with the results of cementitious mortars. We note that, depending on the range of rotational velocities and further details of the fitting routine, the actual values vary.

The model concretes investigated, i.e., MC42-IPF with MF2-1.2% and MC42-TUBAF with MF2-0.8%, are characterised by yield stress and a shear-rate-dependent viscosity; cf. Fig. 5b. Again, the flow curves show behaviour that is more complex than that of a Bingham fluid. However, within the mentioned range of shear rate (1–10 s^{-1}), the model concrete showed a linear behaviour. Similar to model fluid, yield stress and plastic viscosity are estimated for the measurement points within the defined range. The range of rotational velocity (shear rate), within each the rheological properties of real and model systems can be compared, are marked in Figs. 2 and 5. It is worth mentioning that during pumping, the concrete undergoes large shear rates. Therefore, different behaviour of real and model concrete at shear rates lower than 1 s^{-1} do not cause large errors when studying pump flow behaviour and flow-induced particle migration.

As discussed earlier, the actual rheological requirements for the model fluid depend on the size of the glass particles that are explicitly added to the system and on the pipe diameter used. When the concentration of the rheology modifiers is insufficient, i.e., the yield stress is too low and particles can sediment to the bottom of the mixture. Accordingly, the model fluid has to be adapted to the chosen particle sizes. In the paper at hand, the compositions MC42-IPF with MF2-1.2% and MC42-TUBAF with MF2-0.8% were used for further analysis.

Similar to real concrete and mortar, the Bingham model is used to derive the rheological parameters of the model fluid and the model concrete within the shear rate range of 1–10 s^{-1}. The estimates for the Bingham parameters – yield stress and plastic viscosity – for model fluids and (non-segregating) model concretes are summarized in Table 5. These values are compared with the Bingham parameters for cementitious mortar and real concrete; cf. Fig. 6a and b. Thus, in order to attain a target value for yield stress and plastic viscosity in the same range of concrete MC42-TUD, the model fluid requires higher values of yield stress and plastic viscosity in comparison to the cementitious mortar. Certainly, the rheology of the model fluids that replaces the mortar in real concrete depends on the smallest size of the added particles. Since the three model concretes differ in the smallest particle size, the corresponding model fluids accordingly show different rheological properties. A comparison between C42 and MC42-TUD in Tables 2 and 5 reveals similar rheological behaviour for real and model concretes when the model fluid has twice the yield stress and plastic viscosity of mortar. Due to the granular nature of constitutive mortar, i.e., cement, fines and fine sands, the segregation is less pronounced in cementitious concretes. However, the model systems presented here show enough flexibility in their rheological properties to mimic the essential rheological properties of concrete, i.e., yield stress and shear-rate-dependent viscosity.

3.5. Similarity of real and model concrete

In order to judge the performance of the new model concrete, it is useful to check the important dimensionless numbers. Approximating the model concrete similar to the real concrete as a yield stress (Bingham) suspension, the macroscopic behaviour is scaled with the Bingham Reynolds number Re_B and the Hedstrom number He [6].

$$Re_B = \frac{\rho_{eff} U L}{\mu_{pl}} \qquad He = \frac{\rho_{eff} \tau_0 L^2}{\mu_{pl}^2}$$

with the effective density of the suspension ρ_{eff}, the mean velocity U, the characteristic macroscopic length scale of the flow L, the plastic viscosity μ_{pl} and the yield stress τ_0. If concrete C47 is pumped with $U = 0.5$ m/s through a pipeline of diameter $D = 0.1$ m, the dimensionless numbers are $Re_B^{C47} = 5$ and $He^{C47} = 5$. If the pumping process is modelled with model concrete MC42-TUBAF in a pipeline with diameter $D = 0.02$ m and $U = 0.5$ m/s (compare Fig. 10), the values $Re_B^{MC42} = 11$ and $He^{MC42} = 3$ are found.

On the other hand, the microscopic behaviour of individual particles suspended in a Bingham liquid is characterised by the yield number Y and the particle Bingham number Bi_p.

$$Y = \frac{\tau_0}{\left(\rho_p - \rho_l\right) g d} \qquad Bi_p = \frac{\tau_0 d}{\mu_{pl} U}$$

with the particle diameter d, the particle density ρ_p and the liquid density ρ_l, respectively. In a flow of the real concrete with mean velocity $U = 0.5$ m/s, vanishing density difference between cement paste and coarser aggregates, cement plastic viscosity $\mu_{pl} = 1.2$ Pa · s and yield stress $\tau_0 = 20$ Pa, a very large yield number $Y > 1$ and a Bingham number $Bi \approx 0.03$ is found for particles with diameter $d = 1$ mm. For the flow of the model concrete with the same mean velocity, density difference between model cement and glass beads $\rho_p - \rho_l \approx 1100$ kg/m^3, model cement plastic viscosity $\mu_{pl} = 0.3$ Pa · s and yield stress $\tau_0 = 1.8$ Pa, a yield number $Y = 0.16$ and a Bingham number $Bi \approx 0.01$ is found for

Table 5
The Bingham parameters of the model fluid and model concrete for TUD, IPF and TUBAF.

Model fluid	MF1-0.3%	MF2-1.2%	MF2-0.8%
Yield stress [Pa]	41.01	6.85	1.82
Plas. viscosity [Pa·s]	3.71	1.51	0.31
Model concrete	**MC42-TUD**	**MC42-IPF**	**MC42-TUBAF**
Yield stress [Pa]	70.00	26.00	10.30
Plas. viscosity [Pa·s]	22.00	2.65	1.51

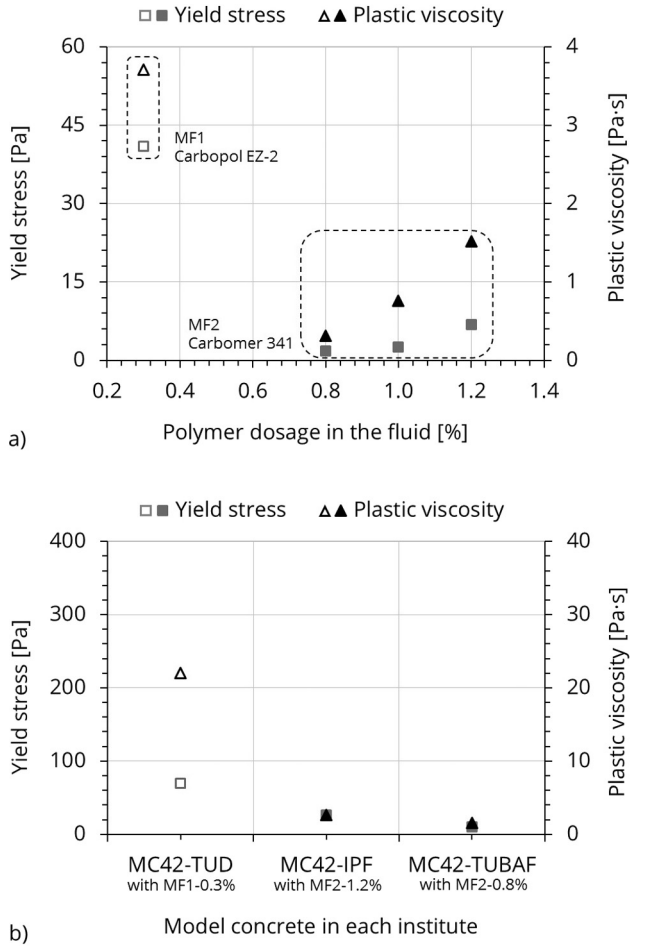

Fig. 6. Comparison between the Bingham parameters of a) mortar and model fluid, b) concrete and model concrete. The yield stress and plastic viscosity are marked on the right and left axis, respectively. Due to the differences in the smallest explicitly added particles to the different model concretes, some differences between the model systems and the real system are expected; see main text for details.

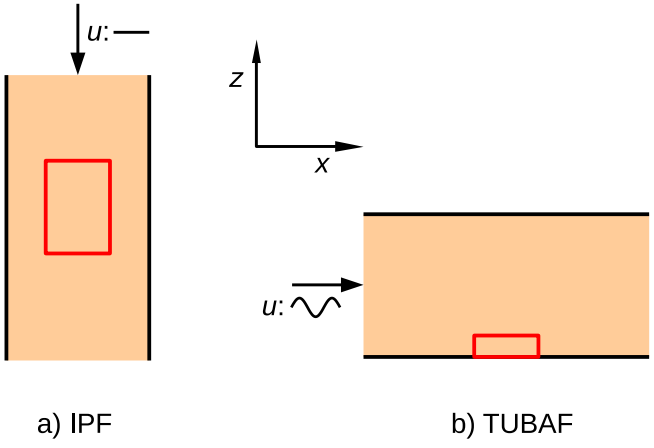

Fig. 7. Flow configurations for measurements with the new model concrete. The flow direction is marked by arrows and the regions of interest are shown in red rectangles.

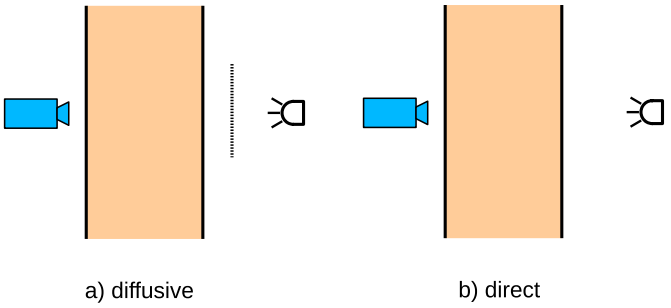

Fig. 8. Illuminations concepts for flow measurements with the new model concrete.

particles with diameter $d = 1$ mm. Therefore, the main differences seem to be in the yield number. The deviation in the yield number for real concrete and the model concrete can be traced back to the fact that the densities of the main constituents in real concrete (aggregates and cement paste) differ less than those of the constituents in the model concrete (glass beads and model fluid). However, the yield number of the model concrete is still higher than the critical yield number $Y > Y_{crit} \approx 0.07$ [6], indicating that there should be no pronounced sedimentation or settling effects in the suspension. The critical yield number denotes the yield number for which the elastic deformation of a non-yielding suspending fluid can prevent the sedimentation of suspended particles despite the difference in the density of both constituents. Please note, that this criterion holds also for particles suspended in yield stress Poiseuille flows [5]. In summary, the new model concrete is found to reasonably match the most important dimensionless numbers of real concrete, if the tunable parameters of the model concrete and the experimental setup are properly chosen.

4. Continuous flow measurements

Our new model concrete is actually used in different flow configurations at IPF and TUBAF; see Fig. 7. The measurements tackle the flow behaviour and the particle dynamics in the pipeline flows of the model concrete. For this purpose, some of the glass beads in the model concrete are marked (black colored). The pipeline materials are matched to the refractive index of the model concrete to allow optical access to the flow. The exemplary results here demonstrate the advantages of our new model concrete.

The flow configuration at IPF, sketched in Fig. 7a, uses a gravity driven flow from container through a vertical pipe of 37 mm inner diameter. This setup allows for a constant flow rate of the model concrete. Model concrete MC42-IPF with 1% black-colored marker particles is used in the experiments. For observation of the tracer particles, diffuse back-light illumination by a bright light source was used in the

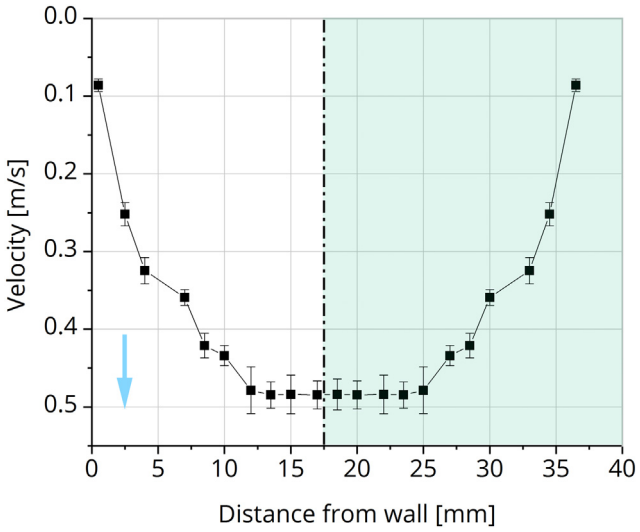

Fig. 10. Flow velocity profile of the particles from particle tracking velocimetry. Only half of the pipe diameter was analyzed (till 18.5 mm, indicated with the centerline). The data in the green shaded area is mirrored of the left side of the graph. The first measurement is at 0.5 mm distance from the wall of the pipe. The blue arrow indicated the flow direction, vertically downwards. The imagining configuration is as indicated in Fig. 7a.

experiments, which allowed the distinguishing of the marked glass beads from the rest of the glass beads and also from the small air bubbles entrained in the model concrete (Fig. 8).

Fig. 9 shows results of the experiments performed with the IPF configuration. As an example, the motions of two glass beads close to each other are marked. The highlighted particles are approximately in the same plane but at a different distance to the pipe wall. The image is taken close the center of the pipe. The particle on the right is in the center of pipe while the particle on the left is nearer the periphery. For a quantitative analysis, we perform particle tracking velocimetry on data sets from the IPF setup.

Fig. 10 shows the flow profile graph for the model concrete in the pipe geometry setup of IPF. Since gravitations acts in this setup parallel to the pipe axis, the sedimentation does not generate an asymmetry in the flow pattern. The velocity of the particle was calculated for the travel distance travelled by the particles in 300 frames. The video was recorded with 2000 fps with a high-speed Photron miniAX200 camera equipped with a Navitar optics with a 2× F-mount and a maximum 12× zoom lens. Transmission illumination was performed with diffuser sheets and a SCHOTT KL 2500 LED. As the video is taken using transmission imaging, particles from different planes are imaged. To obtain the velocities in the center plane of the pipe, only the particles with the highest velocity were taken into account for every distance from the

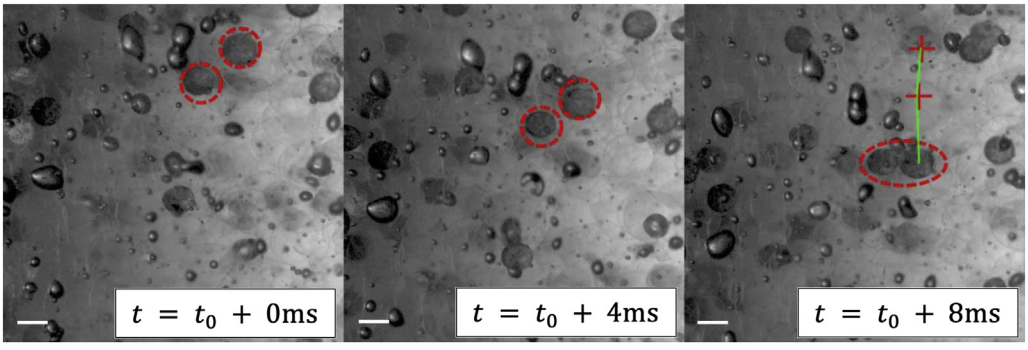

Fig. 9. Motion of tracer particles in the flow experiments of configuration IPF. The images were captured at a frame rate of 250 fps. The diameter of tracer particles is 1 mm. The motion of two particles is marked. The elliptical objects in the images are air bubbles. The scale bar is 1 mm.

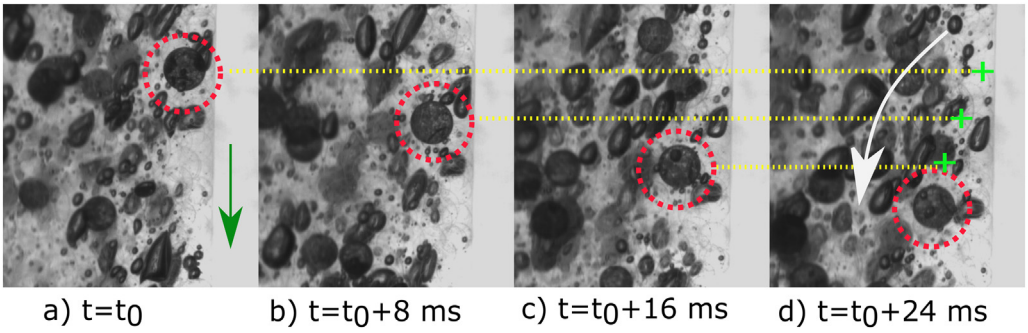

Fig. 11. Particle migration near the wall where the tracer particle appears to be pushed out from the shear flow region and goes into the transition flow region. The tracer particle at t0 in image a is migrating towards the plug flow region in image d. The green arrow indicated the flow direction, vertically downwards, the imagining technique is as indicated in Fig. 7a. The scale is given by the diameter of the tracer particles (1 mm).

wall. The data was analyzed using the standard Particle Tracking Velocimetry (PTV) technique. Particle trajectories were measured using particle tracking feature of the Photron FASTCAM Analysis software (version 1.3.3.0). Near the wall strong shear flow is observed. At a distance of about 10 mm from the wall, a plug flow is observed.

At IPF, as referred in Fig. 11, we have observed migration of particle from the wall of pipe towards the center. This provides qualitative understanding of the movement of particle and particle-particle interaction across the pipe during flow. In comparison to Fig. 12, we observe that the processes close to the wall seem to be relatively independent of the orientation of gravity. This supports the estimates given in Section 3.5.

At TUBAF the flow configuration, sketched in Fig. 7b, aims at tracking the pulsating motion of the model concrete in a horizontal pipeline whose diameter is 20 mm. The setup mimics the pumping process of fresh concrete. Model concrete MC42-TUBAF with 2% of black-colored marker particles was used in the experiments. The measurements were focused on continuum parameters, e.g., the flow velocity in the pipeline, and on segregation processes in the particle phase. Here, direct back-light illumination by a bright LED light source is used in the experiments to distinguish the marked glass beads from the rest of the model concrete. The slightly different illumination facilitates distinguishing the different particle phases. Fig. 12 gives results from flow measurements in configuration TUBAF, where the contact between a larger and a smaller particle at the vicinity of the pipe wall (bottom) is observed. Due to the contact mechanics, the larger particle is driven upwards to the core flow region, whereas the smaller particle remains at the wall. Based on the principal setup of both experiments at IPF and TUBAF, which differ e.g. in orientation with respect to gravity and in the driving mechanism of the flow, different time scales are found in the results shown in Figs. 11 and 12.

To sum up, while studying concrete flow behaviour, such key mechanisms as contacts, segregation and velocity profiles can only be examined by observing the granular suspensions directly. For this, the optical accessibility and transparency of the model concrete in combination with a refractive index matched material system is crucial. Without these features of the model concrete, it would not be possible to get quantitative information from the measurements.

5. Conclusion

In this paper, a new, transparent model concrete with tunable rheological and optical properties is proposed. Rheological tunability is a key feature in mimicking the behaviour of real concrete under processing conditions such as pumping and mixing. Here it is shown that yield stress as well as viscosity can be adjusted by using different amounts of Carbomer®. This allows for producing a material resistant to sedimentation and bleeding.

Furthermore, the material is not only matched to the desired rheology, but its refractive index is matched as well. Critical processes in concrete-like segregation processes near the wall can be observed directly. Additionally, the movement of single particles during pipe flow can be tracked and the velocity field during pumping processes can be determined. For the measurement shown here, the refractive index was matched to that of borosilica glass; different optical properties are, of course, also possible.

The material described in this study is the first to allow for the optical investigation of a dense, granular suspension with non-Newtonian rheology under processing conditions. In the future, this model concrete can be used to study a large variety of technically important processes concerning fresh concrete flow as well as the flow of similar materials.

CRediT authorship contribution statement

Günter K. Auernhammer: Conceptualization, Methodology, Funding acquisition, Project administration, Supervision, Writing - review & editing. **Shirin Fataei:** Conceptualization, Methodology, Data curation, Formal analysis, Investigation, Visualization, Writing - original draft. **Martin A. Haustein:** Conceptualization, Methodology, Data curation, Formal analysis, Investigation, Visualization, Writing - original

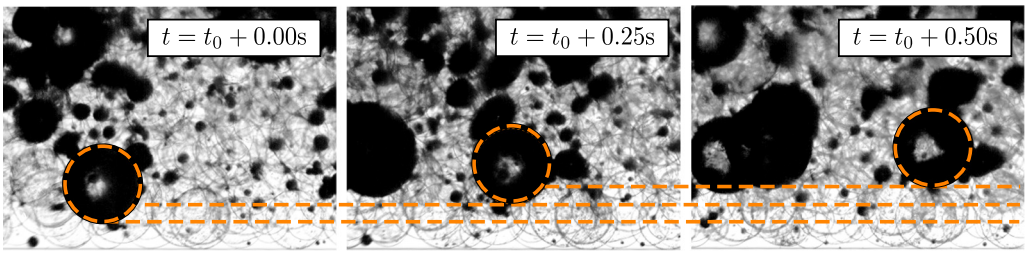

Fig. 12. Segregation in the particle phase near the pipe wall (bottom) in the flow experiments of configuration TUBAF. Near to the pipe wall, only transparent smaller particles are found. Larger particles have a certain distance to the wall, as indicated by the black tracer particle. Furthermore, small entrained air bubbles entrained are clearly visible between the particles. Here, a single, one mm particle moves upwards against gravity in the bulk flow region.

draft. **Himanshu P. Patel:** Conceptualization, Methodology, Data curation, Formal analysis, Investigation, Visualization, Writing - original draft. **Rüdiger Schwarze:** Conceptualization, Methodology, Funding acquisition, Project administration, Supervision, Writing - review & editing. **Egor Secrieru:** Conceptualization, Methodology, Investigation, Project administration, Supervision, Visualization, Writing - original draft, Writing - review & editing. **Viktor Mechtcherine:** Conceptualization, Methodology, Funding acquisition, Project administration, Writing - review & editing, Supervision.

Declaration of competing interest

The authors declare that they have no known competing financial interests or personal relationships that could have appeared to influence the work reported in this paper.

Acknowledgments

Gefördert durch die Deutsche Forschungsgemeinschaft (DFG) – Projektnummern 387100398, 387065607, 387095311, 387153567. Die vier Projekte wurden im Rahmen vom Schwerpunktprogram "Opus Fluidum Futurum – Rheologie reaktiver, multiskaliger, mehrphasiger Baustoffsysteme" (SPP 2005) gefördert; funded by the Deutsche Forschungsgemeinschaft (DFG, German Research Foundation) – project numbers 387100398, 387065607, 387095311, 387153567. The four projects were funded within the framework of the Priority Program "Opus Fluidum Futurum – Rheology of reactive, multiscale, multiphase construction materials" (SPP 2005).

The authors gratefully acknowledge the supply of binder by HeidelbergCement AG and admixtures by BASF. The used Carbomer® was kindly provided by Evonik.

References

[1] B. Andreotti, Y. Forterre, O. Pouliquen, Granular Media: Between Fluid and Solid, Cambridge University Press, Cambridge, 2013.
[2] H. Bauer, Über das Pumpen von Beton durch Rohre mit kleinen Durchmessern, Baumaschine und Bautechnik 7 (1971) 277–281.
[3] C. Bian, Z. Tian, X. Li, J. Xiang, Approach on rheology of ordinary concrete, Earth and Space 2016: Engineering for Extreme Environments , Orlando 2016, pp. 915–925.
[4] B. Boulekbache, M. Hamrat, M. Chemrouk, S. Amziane, Flowability of fibre-reinforced concrete and its effect on the mechanical properties of the material, Constr. Build. Mater. 24 (2010) 1664–1671, https://doi.org/10.1016/j.conbuildmat.2010.02.025.
[5] E. Chaparian, O. Tammisola, Stability of particles inside yield-stress fluid Poiseuille flows, J. Fluid Mech. 885 (2020) A45, https://doi.org/10.1017/jfm.2019.1038.
[6] R. Chhabra, Bubbles, Drops, and Particles in Non-Newtonian Fluids, 2 ed. CRC Press, 2006https://doi.org/10.1201/9781420015386.
[7] M. Choi, N. Roussel, Y. Kim, J. Kim, Lubrication layer properties during concrete pumping, Cem. Concr. Res. 45 (2013) 69–78, https://doi.org/10.1016/j.cemconres.2012.11.001.
[8] F. De Larrard, Concrete Mixture Proportioning: A Scientific Approach, Taylor & Francis Ltd, 1999.
[9] J.A. Dijksman, F. Rietz, K.A. Lörincz, M. van Hecke, W. Losert, Refractive index matched scanning of dense granular materials, Rev. Sci. Instrum. 83 (2012), 011301. https://doi.org/10.1063/1.3674173.
[10] S. Fataei, E. Secrieru, V. Mechtcherine, Influence of aggregate volume fraction on concrete pumping behaviour, Rheology and Processing of Construction Materials, Springer, Cham 2019, pp. 303–310.
[11] H. Giesekus, Phänomenologische Rheologie, Springer-Verlag, Berlin Heidelberg GmbH, 1994.
[12] É. Guazzelli, O. Pouliquen, Rheology of dense granular suspensions, J. Fluid Mech. 852 (2018)https://doi.org/10.1017/jfm.2018.548.
[13] M. Haist, J. Link, D. Nicia, S. Leinitz, C. Baumert, T. von Bronk, D. Cotardo, M.E. Pirharati, S. Fataei, H. Garrecht, C. Gehlen, I. Hauschildt, I. Ivanova, S. Jesinghausen, C. Klein, H.W. Krauss, L. Lohaus, D. Lowke, O. Mazanec, U. Pott, N.W. Radebe, J.J. Riedmiller, H.J. Schmid, W. Schmidt, E. Secrieru, D. Stephan, M. Thiedeitz, M. Wilhelm, V. Mechtcherine, Interlaboratory study on rheological properties of cement pastes and reference substances – comparability of measurements performed with different rheometers and measurement geometries, Mater. Struct. 53 (2020) https://doi.org/10.1617/s11527-020-01477-w (in press).
[14] G. Heirman, R. Hendrickx, L. Vandewalle, D. Van Gemert, D. Feys, G. De Schutter, B. Desmet, J. Vantomme, Integration approach of the Couette inverse problem of powder type self-compacting concrete in a wide-gap concentric cylinder rheometer, Cem. Concr. Res. 39 (2009) 171–181, https://doi.org/10.1016/j.cemconres.2008.12.006.
[15] G. Heirman, L. Vandewalle, D. Van Gemert, Ó.H. Wallevik, Integration approach of the Couette inverse problem of powder type self-compacting concrete in a wide-gap concentric cylinder rheometer, J. Non-Newtonian Fluid Mech. 150 (2008) 93–103.
[16] D. Kaplan, F. de Larrard, T. Sedran, Design of concrete pumping circuit, ACI Mater. J. 102 (2005) 110–117.
[17] J.A. Koch, D.I. Castaneda, R.H. Ewoldt, D.A. Lange, Vibration of fresh concrete understood through the paradigm of granular physics, Cem. Concr. Res. 115 (2019) 31–42, https://doi.org/10.1016/j.cemconres.2018.09.005.
[18] H.D. Le, E.H. Kadri, S. Aggoun, J. Vierendeels, P. Troch, G.D. Schutter, Effect of lubrication layer on velocity profile of concrete in a pumping pipe, Mater. Struct. 48 (2015) 3991–4003, https://doi.org/10.1617/s11527-014-0458-5.
[19] V. Mechtcherine, V.N. Nerella, K. Kasten, Testing pumpability of concrete using Sliding Pipe Rheometer, Constr. Build. Mater. 53 (2014) 312–323, https://doi.org/10.1016/j.conbuildmat.2013.11.037.
[20] V. Mechtcherine, E. Secrieru, C. Schröfl, Effect of superabsorbent polymers (SAPs) on rheological properties of fresh cement-based mortars — development of yield stress and plastic viscosity over time, Cem. Concr. Res. 67 (2015) 52–65, https://doi.org/10.1016/j.cemconres.2014.07.003.
[21] J.F. Morris, Shear thickening of concentrated suspensions: recent developments and relation to other phenomena, Annu. Rev. Fluid Mech. 52 (2020) 121–144, https://doi.org/10.1146/annurev-fluid-010816-060128.
[22] P. Poullain, Etude copmarative de l'ecoulement d'un fluide viscoplastique dans une maquette de malaxeur pour bétons: PIV, IRM et simulation numérique, Ph.D. thesis (in French) Ecole polytechnique de l'Université de Nantes, 2003.
[23] M. Reiner, R. Riwlin, Die theorie der Strömung einer elastischen Flüssigkeit im Couette Apparat, Kolloid-Zeitschrift 43 (1927) 1–5.
[24] J. Spangenberg, N. Roussel, J.H. Hattel, H. Stang, J. Skocek, M.R. Geiker, Flow induced particle migration in fresh concrete: theoretical frame, numerical simulations and experimental results on model fluids, Cem. Concr. Res. 42 (2012) 633–641, https://doi.org/10.1016/j.cemconres.2012.01.007.
[25] E.R. Weeks, J.C. Crocker, A.C. Levitt, A. Schofield, D.A. Weitz, Three-dimensional direct imaging of structural relaxation near the colloidal glass transition, Science 287 (2000) 627–631.
[26] J. Wenzl, R. Seto, M. Roth, H.J. Butt, G. Auernhammer, Measurement of rotation of individual spherical particles in cohesive granulates, Granul. Matter 15 (2013) 391–400, https://doi.org/10.1007/s10035-012-0383-7.
[27] S. Wiederseiner, N. Andreini, G. Epely-Chauvin, C. Ancey, Refractive-index and density matching in concentrated particle suspensions: a review, Exp. Fluids 50 (2011) 1183–1206, https://doi.org/10.1007/s00348-010-0996-8.
[28] S. Zade, T.J. Shamu, F. Lundell, L. Brandt, Finite-size spherical particles in a square duct flow of an elastoviscoplastic fluid: an experimental study, J. Fluid Mech. 883 (2020) A6, https://doi.org/10.1017/jfm.2019.868.